

# Complex Flow of Granular Material in a Rotating Cylinder

Thorsten Pöschel<sup>\*+</sup> and Volkhard Buchholtz<sup>+</sup>

<sup>\*</sup> *HLRZ, Forschungszentrum Jülich, Postfach 1913, D-52425 Jülich, Germany*

<sup>+</sup> *Humboldt-Universität zu Berlin, Institut für Theoretische Physik,  
Invalidenstraße 110, D-10115 Berlin, Germany*

---

## Abstract

The flow of granular material in a rotating cylinder was simulated by molecular dynamics in two dimensions using spherical as well as nonspherical grains. At very low but constant angular velocity we found that the flow varies irregularly with time. The particles move stick-slip like i.e. there are avalanches of different size at the surface of the granular material. Observing the traces of the particles we found that there are unstable convection cells. Our results agree with recent experiments by Rajchenbach [1] and Rolf [2].

---

## 1 Introduction

The flow of granular material in a rotating cylinder is of particular interest since on the one hand it reveals many interesting to physicists phenomena, on the other hand in chemical engineering widely used tumbling ball mills base on the motion of iron spheres moving in rotating cylinders. Hence it has been intensively experimentally subjected by both engineers [2] and physicists [1,3].

The present paper contains results of two dimensional molecular dynamics of grains moving in an uniformly rotating cylinder. Recently Rajchenbach [1] has shown experimentally that the inclination of sand flowing in a rotating cylinder depends nonlinearly on the angular velocity of the cylinder. If the angular velocity is smaller than a certain threshold the sand moves stick-slip like, i.e. there is no continuous flow but there are avalanches of different size, the angle of inclination fluctuates. Using high speed recording of polydisperse iron spheres in a tumbling ball mill Rolf [2] observed that the flow forms convection cells. They found that the size and the number of the cells depend

on the rotation velocity. We will show that our simulations agree with the experimental results [1–3].

Traditional molecular dynamics simulations of granular material use polydisperse spherical grains, examples can be found in [4–6] and many references therein. Applying a recently introduced model for a nonspherical grain [7] which deforms elastically under pressure and dissipates energy during collisions our results agree better with the experiment than the simulations using spheres for the case of low angular velocity. Nonspherical grains in molecular dynamics simulations of granular material have been introduced already by Gallas and Sokołowski [8] in an investigation of the angle of repose of a sand heap. In their model a grain consists of two spheres which are connected by a stiff bar, their results agree with ours.

## 2 Molecular dynamics of granular media

In the simulations we assume that the grains are ideal spheres. To describe the interaction between colliding particles we use a simple Ansatz given by Cundall and Strack [5] and Haff and Werner [6]. Two grains  $i$  and  $j$  at the positions  $\vec{r}_i$  and  $\vec{r}_j$  will interact only if they touch each other, i.e. if the distance between the center points is smaller than the sum of their radii  $R_i$  and  $R_j$

$$|\vec{r}_i - \vec{r}_j| < R_i + R_j \quad . \quad (1)$$

For this case the force between particles  $i$  and  $j$  moving with the velocities  $\dot{\vec{r}}_i$  and  $\dot{\vec{r}}_j$  and rotating with angular velocities  $\dot{\Omega}_i$  and  $\dot{\Omega}_j$  is given by

$$\vec{F}_{ij} = F_{ij}^N \cdot \frac{\vec{r}_i - \vec{r}_j}{|\vec{r}_i - \vec{r}_j|} + F_{ij}^S \cdot \begin{pmatrix} 0 & -1 \\ 1 & 0 \end{pmatrix} \cdot \frac{\vec{r}_i - \vec{r}_j}{|\vec{r}_i - \vec{r}_j|} \quad . \quad (2)$$

with the normal force

$$F_{ij}^N = Y \cdot (R_i + R_j - |\vec{r}_i - \vec{r}_j|)^{\frac{3}{2}} + \gamma_N \cdot m_{ij}^{eff} \cdot |\dot{\vec{r}}_i - \dot{\vec{r}}_j| \quad (3)$$

and the shear force

$$F_{ij}^S = \min\{-\gamma_S \cdot m_{ij}^{eff} \cdot |\vec{v}_{ij}^{rel}|, \mu \cdot |F_{ij}^N|\} \quad . \quad (4)$$

For the relative velocity  $\vec{v}_{ij}^{rel}$  of the particle surfaces one can write

$$\vec{v}_{ij}^{rel} = (\dot{\vec{r}}_i - \dot{\vec{r}}_j) + R_i \cdot \dot{\Omega}_i + R_j \cdot \dot{\Omega}_j \quad . \quad (5)$$

The effective mass of the particles  $i$  and  $j$  is given by

$$m_{ij}^{eff} = \frac{m_i \cdot m_j}{m_i + m_j} \quad , \quad (6)$$

and the resulting momenta  $M_i$  and  $M_j$  for the particles  $i$  and  $j$  are

$$M_i = F_{ij}^S \cdot R_i \quad (7)$$

and

$$M_j = -F_{ij}^S \cdot R_j \quad . \quad (8)$$

$Y$  is the Young modulus,  $\gamma_N$  and  $\gamma_S$  are the phenomenological normal and shear friction coefficients,  $\mu$  stands for the Coulomb friction parameter.

The underlying assumption is that the particles deform each other slightly during collisions. To simulate three dimensional behavior we use the Hertzian contact force [9] which rises with the power 1.5 of the penetration depth  $R_i + R_j - |\vec{r}_i - \vec{r}_j|$ . Eq. (4) takes into account that the particles slide on each other for the case that the inequality

$$\mu \cdot |F_{ij}^N| < |F_{ij}^S| \quad (9)$$

holds, otherwise they roll. This behavior is due to the Coulomb law.

For the integration of Newtons equations of motion due to the forces  $\vec{F}_{ij}$  given above we used a sixth order Gear predictor–corrector algorithm [10]. This high accuracy is necessary since there is a short range interaction between the particles, a small inaccuracy in the calculation of the particle positions may cause large faults in the resulting forces. Using algorithms of lower accuracy the system would become numerical unstable. The calculation of the rotation of the particles is not such sensitive since the angular velocity is very small in general, hence we applied a fourth order algorithm only.

In the simulations we use for the parameters  $Y = 10^4 kg/s^2$ ,  $\gamma_N = 1.5 \cdot 10^4 s^{-1}$ ,  $\gamma_S = 3 \cdot 10^4 s^{-1}$ ,  $\mu = 0.5$ . The radii of the particles are Gauss distributed with the mean value  $\overline{R_i} = 1 mm$ . The chosen parameters are typical for a soft granular material.

The model described above was applied to a simulation of granular material consisting of 2400 single grains moving in a clockwise rotating cylinder of diameter  $160 \cdot \overline{R_i}$ , the cylinder rotates with angular velocity  $\Omega = 0.002 sec^{-1}$ . Fig. 1 shows a snapshot of the simulation.

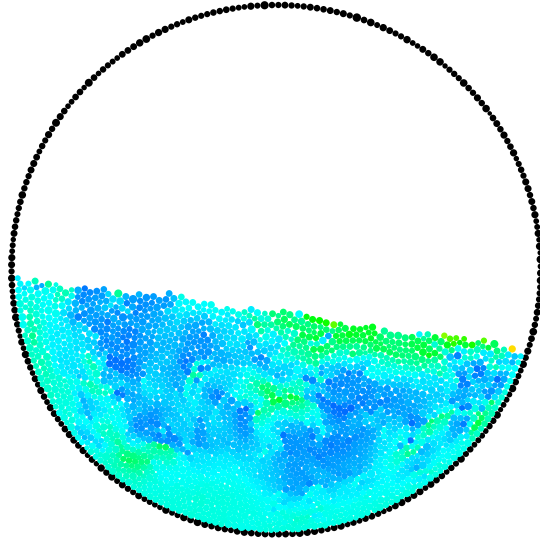


Fig. 1. Snapshot of the simulation of 2400 spherical grains moving in a cylinder which rotates with constant angular velocity  $\Omega = 0.002 \text{ sec}^{-1}$ . High velocity is coded by red color, particles moving with low velocity are drawn blue.

The color codes for the velocity of the particles, slow particles are drawn blue, fast are drawn red. As visible the velocity of the particles near the surface of the flow is nonuniform. The surface of the granular material is close to an even plane which is inclined by an angle  $\Theta \approx 8^\circ$ . Although the dynamics of the flow seems to be very regular the traces of the grains during the simulation are due to convection cells (fig.2). Since there are more than one cell they cannot remain stable over a long time because all of them have the same sense of rotation and therefore they disturb each other. This effect was observed experimentally too in the investigation of tumbling ball mills [2].

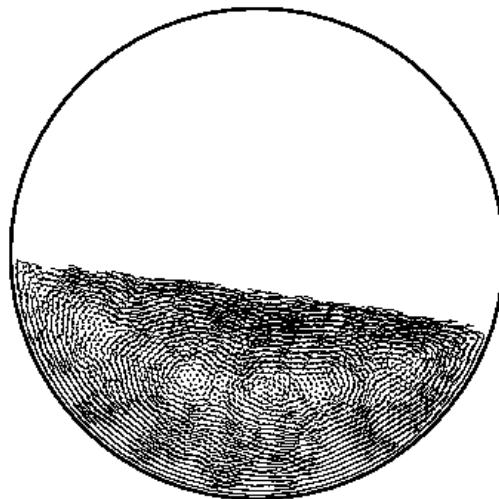


Fig. 2. Traces of the motion of granular material at an angular velocity  $\Omega = 0.002 \text{ sec}^{-1}$ . One observes several unstable convection cells.

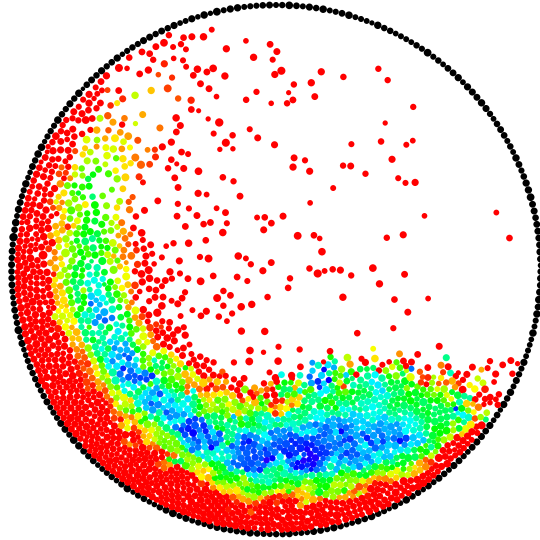


Fig. 3. Snapshot of the simulation of 2400 spherical grains moving in a cylinder which rotates with high angular velocity  $\Omega = 0.1 \text{ sec}^{-1}$ . The bulk of the granular material is S-shaped.

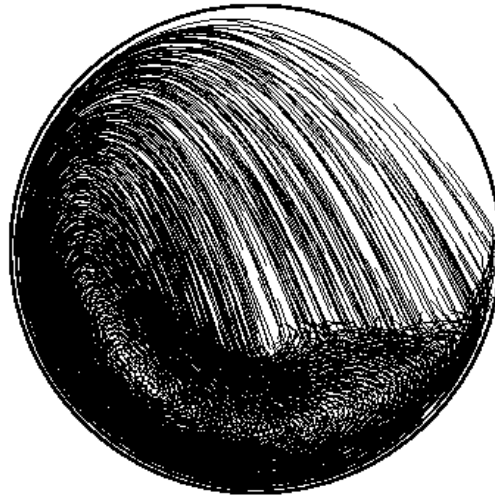


Fig. 4. Traces of the particles for a high angular velocity ( $\Omega = 0.1 \text{ sec}^{-1}$ ). There is only one large convection cell.

Figs. 3 and 4 show a snapshot and the plot of the traces of a simulation with angular velocity  $\Omega = 0.1 \text{ sec}^{-1}$ . The surface of the granular material is not an even plane anymore, but it becomes S-shaped. The same shape characteristic was observed in experiments by Rajchenbach [1]. In the simulations for high angular velocity one finds only one large convection cell (fig. 4) instead of several for lower angular velocity, this behavior is due to the experiment [2].

After submitting this article we received a preprint by Baumann, Jobs and Wolf [11] who applied the interesting simulation method by Visscher and Bolsterli [12] (improved version [13]) to the problem of the rotating cylinder. They

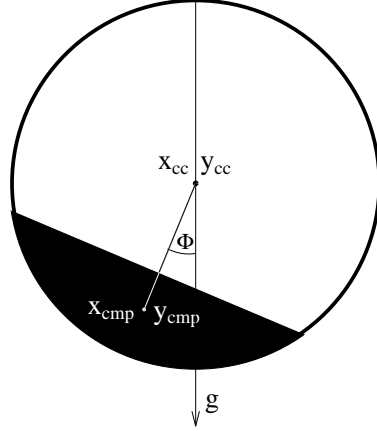


Fig. 5. Schematic description of the procedure we used to determine the inclination  $\Theta$ .

found convection cells as well.

Because the surface of the simulated granular flow is not a perfect plane even for very slow rotation we have to determine the inclination indirectly. It is given by

$$\Theta = \arctan \left( \frac{x_{cc} - x_{cmp}}{y_{cc} - y_{cmp}} \right), \quad (10)$$

where  $(x_{cmp}, y_{cmp})$  are the coordinates of the center of mass point and  $(x_{cc}, y_{cc})$  is the rotation center of the cylinder (fig. 5).

As shown in figs. 1 and 3 the profile of the granular material depends on the angular velocity. Curve (a) in fig. 6 shows the relation between the angular velocity  $\Omega$  and the inclination  $\Theta$ . It rises almost linear with the angular velocity. Using the Ansatz

$$\Theta - \Theta_c \sim \Omega^m \quad (11)$$

we found for the exponent  $m \approx 0.8$  for the interval  $0 < \Omega < 2 \text{ rpm}$ . For larger angular velocities the profile is not close to an even plane but S-shaped.

Although the cylinder rotates with a constant angular velocity the flow of the surface particles varies irregularly with time and space, this behavior is shown in fig. 7. Each horizontal strip of this figure shows the velocity distribution along the surface of the flow. As before red color means high velocity, blue means low velocity. The irregular flow was experimentally observed by Rajchenbach [1] and Briscoe et. al. [3] before. Curves (a) in fig. 9 show the time evolution of the inclination and of the particle velocity at the surface, both values fluctuate irregularly.

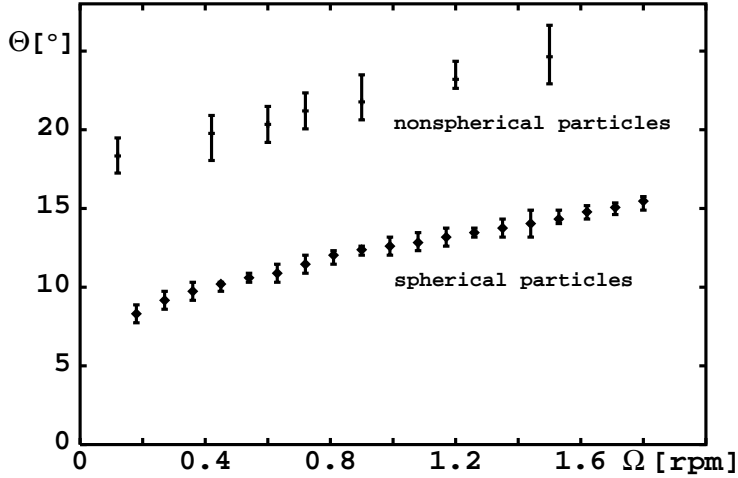


Fig. 6. Inclination  $\Theta$  as a function of the angular velocity  $\Omega$  of the cylinder for spherical (a) and nonspherical (b) grains. In both cases the inclination rises as  $\Theta - \Theta_c \sim \Omega^{0.8}$ , where  $\Theta_c \approx 8^\circ$  for spheres and  $\Theta_c \approx 18^\circ$  for nonspherical particles.

### 3 A more complex model

In the previous section we have shown that the granular flow is irregular, however, fig. 9 proves that there are no sharp bounded avalanches. Experimental observations, however, show that the flow at the surface of granular material in a rotating cylinder is stick-slip like, i.e. there are avalanches of different size going down the surface. Our simulations with spherical grains cannot reproduce this behavior. Hence we apply another model where the grains are not simple spheres but of more complex shape.

Each nonspherical particle  $k$  consists of four spheres of radius  $r_i^{(k)}$  located at the corners of a square of size  $L^{(k)}$  and one additional sphere in the center of the square (fig. 10). The radius  $r_m^{(k)}$  of the middle sphere is chosen to touch the others

$$r_m^{(k)} = L^{(k)}/\sqrt{2} - r_i^{(k)} \quad . \quad (12)$$

During each collision between two spheres  $i$  and  $j$  with radii  $R_i$  and  $R_j$  which might belong to the same grain or to different grains acts a force in normal direction

$$\vec{F}_{ij}^C = \left[ Y(R_i + R_j - |\vec{r}_i - \vec{r}_j|) + \gamma_N m_{ij}^{eff} |\dot{\vec{r}}_i - \dot{\vec{r}}_j| \right] \frac{\vec{r}_i - \vec{r}_j}{|\vec{r}_i - \vec{r}_j|} , \quad (13)$$

where the effective mass is given by eq. (6). The notation is the same as above. In addition each pair of neighboring spheres  $i$  and  $j$  which both belong to the

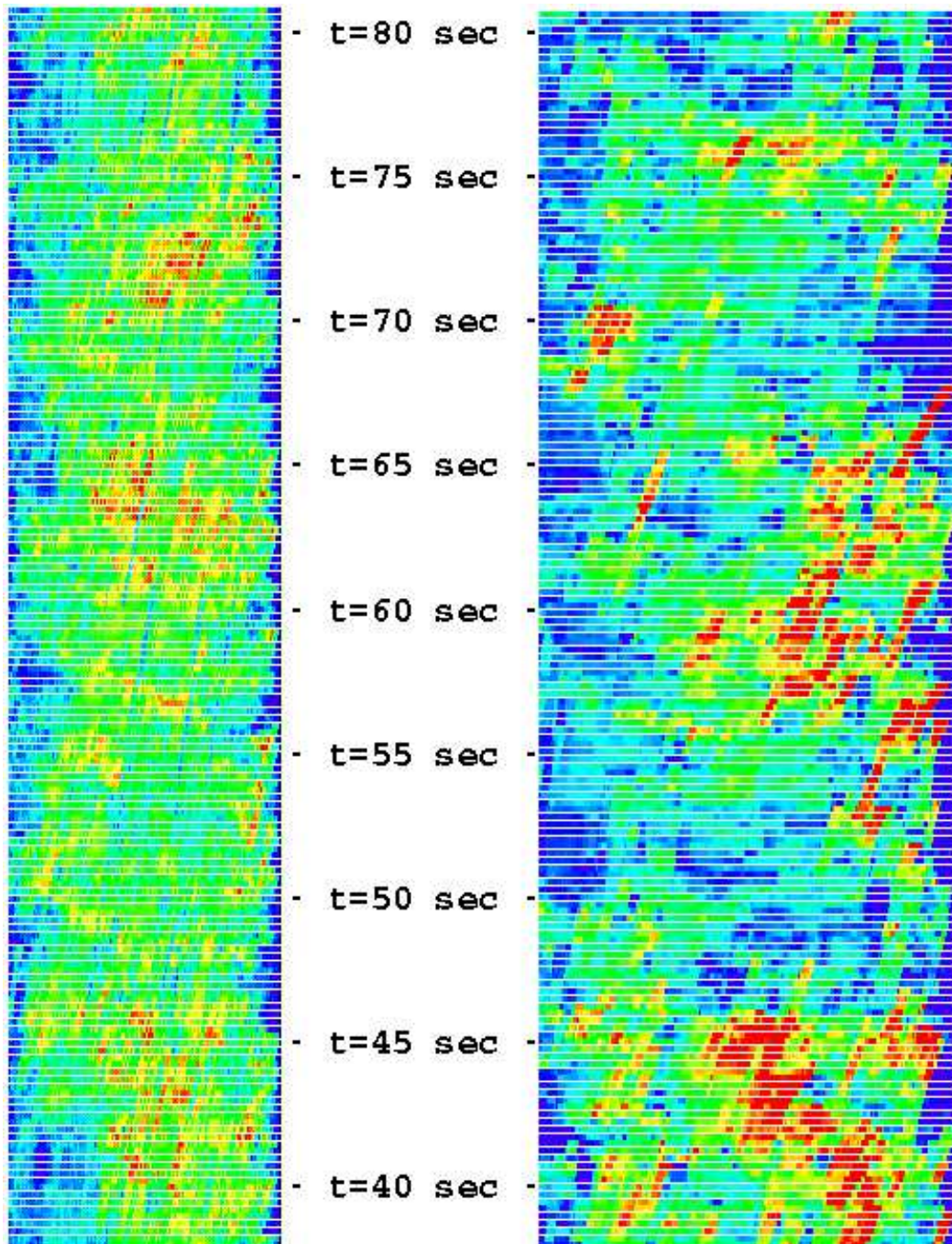


Fig. 7. (left) Evolution of the velocity of the particles moving at the surface of the flow. Each row is a snapshot. The flow varies irregularly in time and space.

Fig. 8. (right) Flow at the surface of the granular material in a simulation using nonspherical grains. There are successive regions of higher and lower energy due to avalanches. The color contrasts are sharper than in fig. 7.



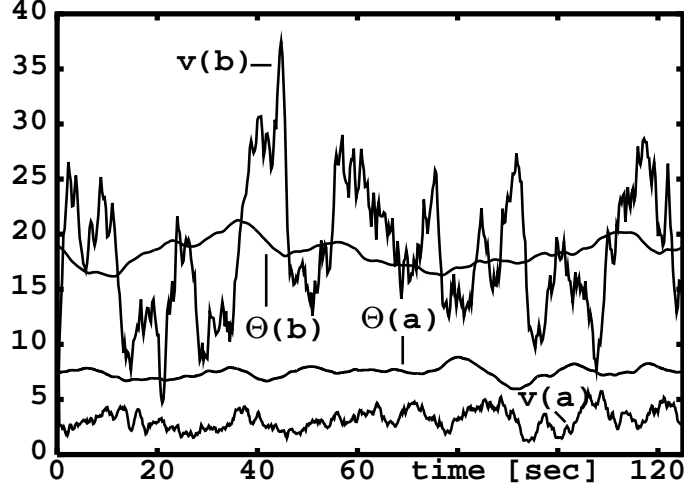


Fig. 9. The inclination  $\Theta[^\circ]$  and the average velocity  $\bar{v}[50 \text{ sec}^{-1}]$  of the surface particles for spherical (a) and nonspherical grains (b). While  $v(b)$  fluctuates drastically due to avalanches  $v(a)$  is much smoother.

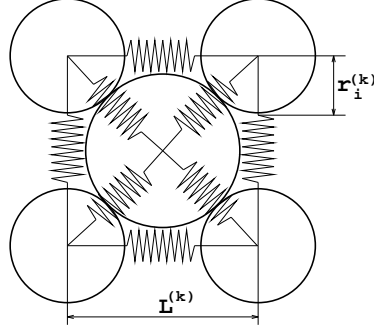


Fig. 10. The nonspherical particles consist of four spheres at the corners of a square and one in the middle of the square which radius is chosen to touch the others.

same grain feel a force  $\vec{F}_{ij}^{Sp}$  due to a damped spring

$$\vec{F}_{ij}^{Sp} = \left[ \alpha(C^{(k)} - |\vec{r}_i - \vec{r}_j|) + \gamma_{Sp} \frac{m_i}{2} |\dot{\vec{r}}_i - \dot{\vec{r}}_j| \right] \frac{\vec{r}_i - \vec{r}_j}{|\vec{r}_i - \vec{r}_j|}, \quad (14)$$

$\alpha$  stands for the spring constant and  $\gamma$  is the damping coefficient. The term  $C^{(k)}$  is the length of the spring in equilibrium

$$C_{ij}^{(k)} = \begin{cases} L^{(k)} & \text{if } i, j \text{ lie at the same edge} \\ L^{(k)}/\sqrt{2} & \text{else} \end{cases}. \quad (15)$$

We want to point out here that eq. (4) which introduces static friction into the interaction forces is not applied in the simulations using nonspherical grains.

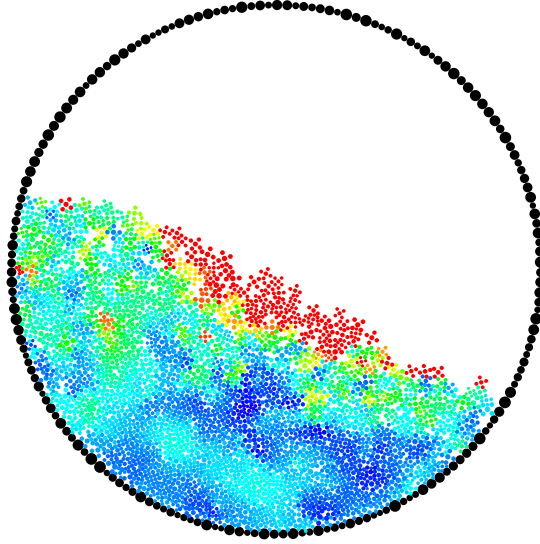


Fig. 11. Snapshot of the simulation of 1000 nonspherical grains each consisting of 5 spheres moving in a cylinder which rotates with constant angular velocity  $\Omega = 0.002 \text{ sec}^{-1}$ . The red drawn grains at the surface show an avalanche.

We investigated the flow of 1000 nonspherical grains, where the parameters are the same as in the previous simulation and  $\alpha = 10^4 \text{ kg/s}^2$ ,  $\gamma_{Sp} = 3 \cdot 10^4 \text{ s}^{-1}$ ,  $L^{(k)}/r_i^{(k)} = 4$  and  $\overline{L^{(k)}} = 3 \text{ mm}$ . The cylinder of diameter  $D \approx 86 \cdot \overline{L^{(k)}}$  rotates with angular velocity  $\Omega = 0.002 \text{ sec}^{-1}$ .

Fig. 11 shows a snapshot of the simulation. Obviously the inclination is approximately twice the inclination observed for spherical grains. The particles at the surface move with much higher velocities than the others. This is due to an avalanche going down the surface in the moment when the snapshot was done.

The equivalent picture to fig. 7 is shown in fig. 8. The flow is irregular in time and space too but one finds time intervals where the surface particles move with high velocities and other intervals where the particle velocities, i.e the flow at the surface, are almost zero. This succession indexes stick–slip motion. The time evolution of the average velocity  $\bar{v}$  of the surface particles and of the inclination  $\Theta$  of the surface for nonspherical (curves(b)) as well as for spherical grains (curves(a)) is drawn in fig. 9. While in the case of spherical grains  $\bar{v}$  varies only slightly for the case of nonspherical particles there are drastic fluctuations of the average velocity due to avalanches of different size.

For the model of nonspherical particles we investigated the dependence of the angle  $\Theta$  of the surface on the angular velocity  $\Omega$  too (fig. 6). The measured inclinations are approximately twice the inclinations observed in simulations with spheres. These values agree better with experimental investigations. For the exponent  $m$  in  $\Theta - \Theta_c \sim \Omega^m$  we found  $m \approx 0.8$ .

## 4 Conclusion

The present paper reports results of two dimensional molecular dynamics simulations of granular material moving in a cylinder which rotates with constant angular velocity. Using spherical particles and the Ansatz of Cundall and Strack [5] for the simulation of static friction we found that the flow fluctuates irregularly with time. The angle  $\Theta$  of the material as well as the velocity of the grains at the surface fluctuate significantly. For the dependence of the inclination  $\Theta$  of the granular material on the angular velocity  $\Omega$  of the cylinder we found  $\Theta - \Theta_c \sim \Omega^{0.8}$ . The flow of the particles forms unstable convection cells. For low rotation velocity we observed several cells, for high rotation velocity we observed only one cell. In the latter case the bulk of the granular flow reveals a typical S-shape.

When using nonspherical grains, where each grain consists of four spheres located at the corners of a square and a fifth sphere at the center, and where neighboring spheres of the grain are connected by a damped spring, we found that the flow moves stick-slip like. That means there are avalanches of different size at the surface of the flow. The inclination of the granular material  $\Theta$  is more than two times larger than in the simulations using spheres which agrees better with the experiment.

In experiments was observed that for low angular velocity  $\Omega$  the particles move stick-slip like due to avalanches going down the inclined surface, for higher velocity one found continuous flow and the characteristic S-shape [1]. The inclination depends nonlinearly on the angular velocity. In experiments with tumbling ball mills unstable convection cells have been observed [2].

Our simulations reproduced the experimentally measured effects using simple assumptions about the behavior of a grain during the collisions. The dynamic effects as irregular flow at low rotation velocity, the finite inclination and the existence of convection cells could be reproduced using simple spherical grains. To simulate the avalanches at the surface of the flow, which is an effect of the static friction between the grains, we applied a more complex model for grains which includes nonsphericity.

## Acknowledgment

The authors thank H. J. Herrmann for helpful discussions.

## References

- [1] J. Rajchenbach, *Phys. Rev. Lett.* **65**, 2221 (1990).
- [2] L. Rolf, *Zement–Kalk–Gips* **46**, 117 (1993).
- [3] B. J. Briscoe, L. Pope and M. J. Adams, *Powder Techn.* **37**, 169 (1984).
- [4] H. J. Herrmann, *Physica A* **191**, 263 (1992); J. A. C. Gallas, H. J. Herrmann, and S. Sokołowski, *Phys. Rev. Lett.* **69**, 1371 (1992); Y. H. Taguchi, *Phys. Rev. Lett.* **69**, 1367 (1992).
- [5] P. Cundall and O. D. L. Strack, *Géotechnique* **29**, 47 (1979).
- [6] P. K. Haff and B. T. Werner, *Powder Technol.* **48**, 239 (1986).
- [7] T. Pöschel and V. Buchholtz, *Phys. Rev. Lett.* **71**, 3963 (1993); V. Buchholtz and T. Pöschel, *Physica A* **202**, 390 (1994).
- [8] J. A. C. Gallas and S. Sokołowski, *Int. J. Mod. Phys. B* **7**, 2037 (1993).
- [9] L. D. Landau, E. M. Lifshits, *Teoriya Uprugosti*, Nauka (Moskva 1965); L. D. Landau, E. M. Lifschitz, *Elastizitätstheorie*, Akademie–Verlag (Berlin 1989).
- [10] M. P. Allen and D. J. Tildesley, *Computer Simulations of Liquids*, Clarendon Press (Oxford 1987); O. R. Walton, R. L. Braun, *J. Rheol.* **30**, 949 (1986).
- [11] G. Baumann, E. Jobs, and D. E. Wolf, In: M. Matsuhita, M. Schlesinger, and T. Vicsek (eds.), *Proc. “Fractals in Natural Sciences”*, World Scientific (Singapore, to appear).
- [12] W. M. Visscher and M. Bolsterli, *Nature* **239**, 504 (1972).
- [13] R. Jullien, P. Meakin, and A. Pavlovitch, *Phys. Rev. Lett.* **69**, 640 (1992); *Europhys. Lett.* **22**, 523 (1993).